For a Research Article in *Nature Communications*

Transcription reinitiation by recycling RNA polymerase that diffuses on DNA after releasing terminated RNA

Wooyoung Kang[1,6], Kook Sun Ha[2,4,6], Heesoo Uhm[1,5], Kyuhyong Park[1], Ja Yil Lee[3], Sungchul Hohng[1,7]*, Changwon Kang[2,7]*

[1]Department of Physics and Astronomy, and Institute of Applied Physics, Seoul National University, Seoul 08826, Republic of Korea. [2]Department of Biological Sciences, Korea Advanced Institute of Science and Technology, Daejeon 34141, Republic of Korea. [3]School of Life Sciences, Ulsan National Institute of Science and Technology, Ulsan 44919, Republic of Korea. [4]Present address: Department of Life Science, University of Suwon, Gyeonggi-do 18323, Republic of Korea. [5]Present address: Department of Physics, University of Oxford, Oxford OX1 3PU, United Kingdom. [6]These authors contributed equally: Wooyoung Kang, Kook Sun Ha. [7]These authors jointly supervised this work: Sungchul Hohng, Changwon Kang.
*Correspondence and requests for materials should be addressed to C.K. (email: ckang@kaist.ac.kr) or S.H. (email: shohng@snu.ac.kr)

Words in the title (≤15): 14
Words in the Abstract (≈150): 144
Words in the Introduction, Results, Discussion and Methods sections (≤5,000): 4,116
Words in the Methods section alone (≤3,000): 1,571
Display items (≤10): 4 color figures and 0 tables
Words in figure legends (≤350 each): 129, 111, 87 and 84
References (≤70): 26
Supplementary information: Tables S1 to S4 and Figures S1 to S7

(Abstract)
Despite extensive studies on transcription mechanisms, it is unknown how termination complexes are disassembled, especially in what order the components dissociate. Our single-molecule fluorescence study unveils that RNA transcript release precedes RNA polymerase (RNAP) dissociation from DNA template in bacterial intrinsic termination of transcription much more often than concurrent dissociation. As termination is defined by release of product RNA from transcription complex, the subsequent retention of RNAP on DNA constitutes a previously unidentified stage, termed here as 'recycling.' During the recycling stage, RNAPs one-dimensionally diffuse on DNA in downward and upward directions, and these RNAPs can initiate transcription again at nearby promoters in case of retaining a sigma factor. The efficiency of this event, termed here as 'reinitiation,' increases with supplement of a sigma factor. In summary, after releasing RNA product at intrinsic termination, recycling RNAP diffuses on DNA template for reinitiation most times.

(introduction)
Gene expression is regulated at not only initiation but also elongation and termination stages of transcription process for RNA biosynthesis, among other subsequent processes such as RNA processing and transport, and protein synthesis, processing, and targeting [1, 2]. Transcription is terminated with particular RNA sequences that are encoded by terminators in DNA template to effect particular pause of RNA polymerase (RNAP) and eventual disassembly of transcription complexes to release RNA product.

For example, in *Escherichia coli* transcription, RNA structures with a GC-rich hairpin followed by a U-rich tract cause intrinsic (factor-independent) termination, which occurs without any factors although its termination efficiency can be affected by some factors [3–6]. The U-rich tract makes elongation complex pause to allow for GC-rich RNA hairpin formation that effects conformation changes to destabilize the complex.

Although the structural changes have not been characterized yet, all termination models [7, 8] include a structural change where DNA·RNA hybrid becomes unstable, which allows RNA to get locally separated from DNA and form hairpins. Single-molecule experiments using optical tweezers have shown that termination mechanisms such as

59 hypertranslocation and shearing mechanisms are terminator-specific [9].

60 However, it is still unknown yet how the complex is broken apart. Especially, which of
61 the three components departs the transcription complex first, RNAP enzyme, RNA product,
62 DNA template, or all together at once? To examine the temporal order of their dissociations
63 and their post-terminational fates in *E. coli* intrinsic termination, we primarily used single-
64 molecule fluorescence measurements.

65

66 **Results**

67 **Construction of fluorescent transcription complex.** A primary DNA template (Figure 1A)
68 was synthesized to consist of a 50-bp upstream part including the strong promoter A1 of
69 bacteriophage T7, a 38-bp transcription unit with the intrinsic terminator tR2 of phage λ,
70 and a 15-bp downstream part. It was pre-labeled with Cy5 at the 5' end of template strand
71 (downstream end) and additionally with biotin at the 5' end of nontemplate (coding) strand
72 (upstream end).

73 In an experiment with radioactive UTP, the major termination site (TS) was +38 position
74 relative to the transcription start site +1, and termination efficiency was 39%. This double-
75 labeled template with a TS-downstream length of 15 bp is denoted by L+15. Likewise, other
76 DNA templates are denoted by L+# with TS-downstream base-pair numbers.

77 A fluorescent transcription complex with Cy3-labeled RNA was prepared by incubating
78 L+15 with Cy3-labeled ApU, ATP, CTP, GTP, and *E. coli* RNAP holoenzyme with σ^{70} for 30 min
79 in a transcription buffer (Figure 1B). Transcription is initiated preferentially with Cy3-ApU,
80 which is incorporated into the +1 and +2 positions of RNA, but stalled at +12 waiting for the
81 missing UTP. The stalled complexes were immobilized on polymer-coated quartz slides using
82 biotin-streptavidin conjugation.

83

84 **Fluorescent detection of termination and readthrough.** The synchronized, immobilized
85 complexes were then subjected to resumption of elongation by adding all four
86 ribonucleotides (NTPs), while fluorescence images of Cy3-RNA and Cy5-DNA in individual
87 complexes were monitored using total internal reflection fluorescence microscopy. The
88 resumed elongation is followed by either readthrough or termination at TS leading to

89 continued or discontinued downstream transcription, respectively. In the fluorescence
90 images (Figure 1C), vanishing of Cy3-RNA images from the Cy5-DNA spots after NTP addition
91 indicates release of RNA from immobilized DNA, which defines termination of transcription.
92 In readthrough events, the terminator is ignored by RNAP that passes through TS and
93 continues to transcribe its downstream. With readthrough complexes, from which Cy3-RNA
94 signal is not vanished, protein-induced fluorescence enhancement (PIFE) of Cy5 occurs with
95 red laser excitation (Figure 1D), indicating that RNAP reaches the downstream end of DNA
96 and contacts Cy5 there [10]. Additionally, fluorescence resonance energy transfer from Cy3
97 to Cy5 occurs with green laser excitation, indicating that the 5' end (Cy3) of RNA also
98 approaches the downstream end (Cy5) of DNA presumably due to cotranscriptional folding
99 of RNA.
100 In termination events, the terminator is recognized by RNAP that ends elongation at TS
101 and does not transcribe its downstream. From termination complexes, Cy3-RNA signal
102 vanishes 4.3±0.3 s after NTP addition (Figure 1E). The termination efficiency measured by
103 frequency of this pathway is 34±4%, similar to the above measured using radioactive
104 incorporation. When ITP is used instead of GTP to destabilize terminator hairpin RNA, this
105 pathway is reduced to 10±1%. Furthermore, this pathway is not observed with a terminator-
106 lacking template L+15M.
107
108 **RNAP remaining on DNA after releasing RNA.** Surprisingly, Cy5 PIFE is observed in most
109 (91%) of the termination complexes (Figure 1E). The PIFE starts almost concurrently with
110 Cy3-RNA vanishing and is maintained for 536±82 s (Figure S1), while Cy5 photobleaching
111 takes a much longer time of 2350 s (Figure S2). Accordingly, after termination, most RNAPs
112 keep contacting DNA, as its possibility was previously speculated [11]. This was additionally
113 observed with other intrinsic terminators (Table S3) such as *E. coli his* operon attenuator
114 (87%) and phage ϕ82 t500 terminator (70%), suggesting that the post-terminational
115 retention of RNAP on DNA is general.
116 To gain further support, we repeated the experiments with Cy5 placed on σ factor
117 rather than DNA (Figure 1F), because the initiation factor has been recently reported to
118 remain in some elongation complexes [12, 13]. *E. coli* σ^{70} was labeled with Cy5 at Cys-336 as

119 previously described [14]. Cy5-σ is retained in 75% of the initially-stalled complexes (Figure
120 S3), which falls within a previously reported 70-90% range of σ retention [13].
121 This Cy5-σ of holoenzymes mostly (84%) remain on immobilized DNA even after Cy3-
122 RNA vanishing of termination (Figure 1G). In no cases, Cy5-σ vanishes before Cy3-RNA. The
123 dissociation time of σ^{70} (588±85 s, Figure S4) is similar to that of RNAP (536±82 s, Figure S1),
124 suggesting that the holoenzyme maintains a stable complex throughout its retention on
125 DNA.
126
127 **One-dimensional diffusion of RNA-free RNAP on DNA.** After releasing RNA, RNAP can reach
128 the Cy5-end of DNA through three-dimensional (3D) diffusion after dissociation from DNA or
129 through one-dimensional (1D) diffusion (sliding or hopping) without dissociation from DNA.
130 To examine how RNA-free RNAP reaches DNA ends, a recognition sequence of EcoRI
131 restriction enzyme was inserted into DNA at downstream of TS (Figure 2A). DNA-bound
132 EcoRI blocks procession of *E. coli* RNAP [15], so this roadblock would obstruct 1D diffusion
133 downward from TS, but not TS-upward 1D diffusion or 3D diffusion.
134 In experiments using a cleavage-lacking mutant E111Q of EcoRI [16], this roadblock
135 reduces PIFE occurrence among the termination complexes when Cy5 is placed at the
136 downstream end of L+112 (from 89±2% to 25±7%), but not with Cy5 placed at the upstream
137 end of L+112R (Figures 2A and 2B). As the PIFE occurrence reduction is as much as DNA
138 cleavage inhibition by E111Q (71±5%; Figure S5), the Cy5-ends are reached by RNAP mostly
139 through 1D diffusion, much more often than 3D diffusion.
140
141 **Post-terminational diffusion lifetime of RNAPs.** It is known that RNAP preferentially binds
142 blunt ends of DNA, so the post-terminational retention time of RNAP or σ on short DNA
143 molecules could be longer than the 1D diffusion lifetime, which can be measured on long
144 DNA molecules where diffusing RNAP takes too long to reach an end. The σ-retention time
145 (Cy5 signal duration) after termination was measured on a long DNA of 1560 bp with 6.4%
146 of PIFE occurrence expectation.
147 The post-terminational diffusion of RNAP lasts for 75±5 s on this long DNA (Figure S6).
148 This lifetime is clearly shorter than RNAP's association with a short DNA of 103 bp at Cy5-

149 end (Cy5-PIFE duration of 536±82 s; Figure S1) or similar association of Cy5-σ holoenzyme
150 with the short DNA (Cy5 signal duration of 588±85 s; Figure S4). RNAP is thus apparently
151 trapped for an extended period once it reaches the ends of DNA.
152
153 **Post-terminational diffusion coefficient of RNAPs.** The 1D diffusion coefficient of post-
154 terminational RNAPs can be estimated by the correlations that Cy5 PIFE starts later and
155 occurs less frequently as the Cy5-end is placed further away from TS (Figures 2C and 2D).
156 Cy5 PIFE was measured with six templates, L+15, L+62, L+112, L+212, L+312, and L+512,
157 where the distance between TS and Cy5-end of DNA (TS-downstream length) varies from 15
158 to 512 bp (Figure 2A).
159 Termination efficiency (ranging from 31±3% to 36±16%) or timing (ranging from 4.0±0.8
160 to 7.1±1.3 s) is little affected by the TS-downstream length (Table S1; Figure S7). On the
161 other hand, with increasing TS-end distance, the PIFE start delay increases from 1.8±0.5 to
162 30±19 s since RNA release (Figure 2C), and the PIFE occurrence decreases from 91% to 47%
163 (Figure 2D), both supporting for 1D diffusion of RNAP on DNA after termination.
164 RNAP diffusion on DNA is modeled to occur with one reflecting end on the surface side
165 and the other absorbing end on the buffer side, which is reasonable because PIFE
166 occurrence at free ends is highly probable with short DNA molecules. This 1D diffusion
167 model adopting the above-determined post-terminational diffusion lifetime of RNAPs fits
168 well to the correlation of the PIFE start timing (R^2 = 0.94) or occurrence (R^2 = 0.96) with the
169 TS-end distance (Figure 2C and 2D), from which the diffusion coefficient is estimated as
170 3.5×10^{-4} or 3.4×10^{-4} $\mu m^2/s$, respectively (see the STAR Methods).
171 On the other hand, the PIFE occurrence data do not fit to a previously described 3D
172 diffusion model [17] (Figure 2D). The PIFE occurrence at zero distance can be additionally
173 estimated by the above 1D diffusion model, and 94% of complexes are estimated to retain
174 RNAP at the time of RNA release at TS, and the remaining 6% release RNAP together with
175 RNA.
176
177 **Transcription reinitiation by post-terminational RNAPs.** During post-terminational diffusion
178 on DNA, RNA-free holoenzymes of RNAP could initiate transcription again when they

179 encounter a promoter. Even core enzymes of RNAP could do so if they become adequately
180 complemented with σ. Here 'reinitiation' refers to another round of promoter binding and
181 initiation by the RNAP that has released RNA but not fallen off DNA and diffuses on DNA
182 rather than by 3D association of RNAP.

183 Reinitiation was examined using a template with two transcription units (Figure 3A).
184 L+15 containing a short transcription unit was extended downstream to contain a roadblock
185 site and another long transcription unit, among other extensions. As explained above, short
186 transcripts from the upstream unit can be labeled with Cy3-ApU, which reports whether
187 termination or readthrough occurs at TS. Long transcripts from the downstream unit contain
188 five repeating 21-bp sequences, and can be probed by a Cy5-labeled DNA oligomer
189 complementary to the repeat sequence.

190 Three courses can proceed (Figure 3B) as they were observed in different types of
191 fluorescence time-traces (Figure 3C). First, reinitiation on the downstream unit occurs after
192 termination from the upstream unit, as Cy5-oligomer probing signal follows Cy3-RNA signal
193 vanishing (type 1). Second, dissociation of RNAP occurs after TS termination, as no Cy5
194 probing follows Cy3 vanishing (type 2). Third, readthrough occurs for continued
195 downstream transcription, as Cy5 probing follows Cy3 nonvanishing (type 3). The relative
196 frequencies of types 1, 2, and 3 were 0.10±0.05, 0.41±0.10, and 0.49±0.12, respectively.

197 Because transcript probing was not complete, not all readthrough events were counted,
198 and some reinitiation events were observed as type 2 instead of type 1. However, using the
199 measured termination efficiency (34%), the probing efficiency was estimated as 49%,
200 allowing the reinitiation (0.21) and dissociation (0.30) events to be re-sorted as described in
201 the Methods. Thus, the reinitiation portion among the termination events was 41% with a
202 mixture of holoenzymes and core enzymes. The reinitiation efficiency decreases to 19% with
203 the above-mentioned roadblock, but increases to 59% with addition of 3 μM σ^{70}.

204

205 **Discussion**

206 This study discovered that RNA transcript is released first from transcription complex, and
207 RNAP dissociates from DNA template much later most times in *E. coli* intrinsic termination,
208 based on our single-molecule monitoring of fluorescent RNA transcript, DNA template or σ

209 factor. This sequential release (94%) is much more frequent than their concurrent
210 dissociation (6%). Considering that only 75% of elongation complexes retained σ factor in
211 our case, the post-terminational retention of RNAP on DNA seems to occur similarly with
212 both core and holoenzymes. Additionally, we showed that most holoenzymes retain the σ
213 factor after termination.

214 Because termination should refer to RNA release only, the subsequent retention of
215 RNAP on DNA constitutes a previously unidentified stage. This fourth stage of transcription
216 after the initiation, elongation, and termination stages is here termed as 'recycling' (Figure
217 4). During the recycling stage, post-terminational RNAPs apparently diffuse on DNA one-
218 dimensionally in downward and upward directions.

219 One-dimensional diffusion of RNAP has been suggested to accelerate promoter search
220 [18-20], but few experiments have directly proved it. Furthermore, RNAP diffusion on DNA
221 was recently measured to be too short (<30 ms) to contribute to initiation kinetics under
222 physiological conditions [21]. This lifetime of pre-initiational RNAP on DNA is much shorter
223 than that of post-terminational RNAP (>1 min) observed in this study, suggesting that their
224 conformations are distinct from each other. Our single-molecule detection of such long and
225 frequent (95%) retention of post-terminational RNAP on DNA provides the first direct
226 evidence that 1D diffusion of RNAP can dramatically accelerate the promoter search process
227 at least *in vitro*.

228 RNAP's post-terminational retention of σ and diffusion on DNA allow for transcription
229 reinitiation, which is defined to occur by promoter binding through 1D rather than 3D
230 diffusion of RNAP. Reinitiation is demonstrated here to occur on a downstream promoter
231 oriented in the same direction with the upstream promoter. Although it is not known yet
232 whether 1D-diffusing RNAP can flip to reinitiate at an oppositely oriented promoter, RNAP
233 can diffuse backward or upward towards the upstream end of DNA. Furthermore, σ
234 supplement is shown here to increase the reinitiation efficiency, suggesting that even core
235 enzyme can become reinitiation-competent during the recycling stage, which ends with
236 reinitiation or dissociation of RNAP.

237 Post-terminational retention and diffusion of RNAP on DNA and transcription
238 reinitiation competence of such RNAP during the recycling stage have several functional

239 implications, although they have not been observed to occur *in vivo* yet. First, they would
240 facilitate transcriptional burst, which has been observed for both bacterial and eukaryotic
241 transcriptions [22-24]. Post-terminational retention of RNAP on DNA during the recycling
242 stage may increase its local density and render it readily convertible into reinitiation-
243 competent state, contributing to the transcriptional burst.
244 Second, simultaneous transcriptional regulation of multiple operons can be facilitated.
245 In bacterial genomes, functionally related genes and operons are often clustered and
246 regulated together as a regulon [25-28]. One can hypothesize that a single RNAP molecule
247 continually transcribes clustered operons while diffusing on inter-operon regions of DNA
248 chromosome.
249 Third, transcriptional memory can be facilitated by recycling RNAPs. A loop formed
250 between promoter and terminator is observed in some eukaryotic genes, although not yet
251 in bacterial operons. Such loops can increase initiation efficiency and provide transcriptional
252 memory [29-31], where facilitated diffusion of RNAPs on the loop could speed up
253 reactivation.
254 In this work, we established a single-molecule fluorescence assay to study bacterial
255 transcription termination dynamics. Our construction of fluorescent transcription complexes
256 can permit single-molecule monitoring of their components in studies on transcriptional
257 elongation, termination, recycling, and reinitiation.
258
259 **Methods**
260 **Preparation of transcription templates.** All transcription templates were prepared by
261 polymerase chain reactions using AccuPower ProFi Taq PCR premix from Bioneer, Korea
262 with the amplification templates and primers purchased from Integrated DNA Technologies,
263 USA. Their sequences are listed in table S3. All amplification products were purified using
264 the Cleanup kit Expin PCR SV mini from GeneAll, Korea.
265 DNA template L+15 was prepared using UP8_template, 5' biotin-labeled
266 forward_primer_ biotin, and 5' Cy5-labeled reverse_primer_L+15; L+15M using
267 UP8M_template, 5' biotin-labeled forward_primer_biotin, and 5' Cy5-labeled
268 reverse_primer_L+15M; L+62 using UP8_template, 5' biotin-labeled forward_primer_biotin,

269 and 5' Cy5-labeled reverse_primer_L+62; L+112 using UP8_template_2, 5' biotin-labeled
270 forward_primer_biotin, and 5' Cy5-labeled reverse_primer_ L+112; and L+112R using
271 forward_primer_Cy5' and reverse_primer_biotin instead. Template for phage ϕ82 t500
272 terminator was prepared using t500_template, 5' biotin-labeled forward_ primer_biotin,
273 and 5' Cy5-labeled reverse_primer_L+62; and template for *E. coli his* operon attenuator
274 using his_template, 5' biotin-labeled forward_primer_biotin, and 5' Cy5-labeled
275 reverse_primer_L+62.
276 For L+212 and L+312 constructions, L+112 and additional_part_1 were annealed with
277 DNA_splint_1 by cooling from 90°C to 30°C for 120 min in the annealing buffer (10 mM Tris-
278 HCl, pH 8.0, with 50 mM NaCl), ligated using T4 DNA ligase 2 purchased from New England
279 Biolabs (NEB), USA, and used for amplification reactions. L+212 was prepared using
280 forward_primer_ biotin and reverse_ primer_L+212; L+312 using forward_primer_biotin
281 and reverse_primer_ L+312. For L+512 construction, L+312 and additional_ part_2 were
282 annealed with DNA_splint_2 and the same ligation reaction was repeated. L+512 was
283 prepared using forward_primer_biotin and reverse_primer_L+512.
284 For templates used for reinitiation detection and σ retention time estimation, long_tail
285 template with HindIII recognition sequence was prepared using lambda DNA (NEB),
286 lambda_forward_primer, and lambda_reverse_primer. To construct the upstream part of
287 reinitiation template, L+112_α was prepared with UP8 template_2,
288 forward_primer_extension, and 5' reverse_primer_L+112. L+112_α and reinitiation_part_1B
289 were annealed with DNA_splint_reinitiation by cooling from 90 to 30 °C for 120 min in the
290 annealing buffer, and the same ligation reaction was repeated. Long_tail DNA, the upstream
291 part of reinitiation template, and L+512 were each digested with HindIII (NEB) for one h at
292 37 °C in the CutSmart™ buffer (NEB). After that, HindIII was deactivated for 20 min at 80 °C.
293 Long_tail DNA were annealed with cleaved L+512 or the upstream part of reinitiation
294 template by the same protocol as above and used for amplification reaction. L+lambda was
295 prepared using forward_primer_biotin and lambda_forward_primer. DNA template for
296 reinitiation detection was prepared using forward_primer_biotin_α and lambda_reverse_
297 primer.
298

299 **Preparation of Cy5-labeled σ factor.** An N-terminal His_6-tagged *E. coli* σ^{70} was produced in
300 BL21(DE3) cells at 25 °C. Soluble fractions of cell lysates were purified by a 5-ml HisTrap
301 column (GE Healthcare) followed by a 5-ml HiTrap heparin column (GE Healthcare). Purified
302 σ^{70} was incubated with Cy5 maleimide mono-reactive dye (1 mM, GE Healthcare) in the
303 storage buffer (50 mM Tris-HCl, pH 8.0, 100 mM NaCl, and 0.1 mM EDTA) overnight at room
304 temperature. Unreacted Cy5-maleimide molecules were removed using an Amicon ultra
305 centrifugal filter (Merck).
306
307 **Single-molecule transcription termination experiments.** To construct a transcription
308 complex, we incubated DNA template (50 nM) with *E. coli* RNAP holoenzyme (20 nM, NEB),
309 ATP, GTP, CTP (20 µM each, GE Healthcare), and Cy3-labeled ApU (250 µM, TriLink) for 30
310 min at 37 °C. For the experiments with Cy5-labeled σ, we used *E. coli* RNAP core enzyme (20
311 nM, NEB) plus 1 µM Cy5-σ instead of RNAP holoenzyme. Quartz slides were cleaned using
312 piranha solution to remove organic residues, incubated with (3-
313 aminopropyl)trimethoxysilane (United Chemical Technologies), and coated with polymers
314 by incubating the slides in a 1:40 mixture of biotin-PEG-5000 and m-TEG-5000 (Laysan Bio).
315 The slides were treated with streptavidin (0.2 mg/ml, Invitrogen) for 5 min, and
316 transcription complexes were immobilized on the surface of quartz slides via biotin-
317 streptavidin conjugation.
318
319 **Single-molecule fluorescence imaging.** A home-made total-internal-reflection fluorescence
320 microscope is equipped with a 532-nm green laser (EXLSR-532-50-CDRH, Spectra-physic) for
321 Cy3 excitation and with a 640-nm red laser (EXLSR-635C-60, Spectra-physic) for Cy5
322 excitation. An electron multiplying charge-coupled device camera (Ixon DV897, Andor
323 Technology) was used as an imaging device and controlled by using a customized C#
324 program. All experiments were performed at 37 °C with 0.05 s exposure time. The time
325 resolution of the experiments was 0.1 s because we used the alternating laser excitation
326 (ALEX) mode.
327 All experiments were performed with an oxygen scavenging buffer (10 mM Tris-HCl, pH
328 8.0, 20 mM NaCl, 20 mM $MgCl_2$, 1 mM dithiothreitol, 5 mM 3,4-protocatechuic acid, and

329 100 nM protocatechuate-3,4-dioxygenase) and 200 µM NTP each. In the roadblock
330 experiments, the immobilized transcription complexes were incubated with E111Q (1 nM)
331 for 10 min, and DNA templates without E111Q were digested using wild-type EcoRI (10
332 units/µl, Beams Biotechnology). Then, we performed the experiments in the oxygen
333 scavenging buffer containing 1 nM E111Q.
334
335 **Single-molecule transcription reinitiation experiments.** The imaging buffers before and
336 after NTP injection contained the same concentration of Cy5-labeled 'imager DNA' (50 nM,
337 Cy5-TGTGT GTGGT CTGTG GTGTC T) to maintain the same background level. From our
338 analysis were excluded the traces that showed Cy5 signal before NTP addition (nonspecific
339 probing). Because tR2 termination occurs at 4.3 s after NTP addition on average, only Cy3
340 vanishing within 15 s was regarded as termination. Among these traces, we classified those
341 with Cy5 probing within 240 s as type 1 and the others as type 2. On the other hand, those
342 with Cy3 surviving longer than 180 s and Cy5 probing within 240 s were classified as type 3.
343 Other traces were excluded from data analysis. The exclusion due to Cy3 survival within the
344 range of 15 to 180 s was minor (11%). The exposure time of 0.2 s was used to reduce
345 photobleaching.
346
347 **One-dimensional diffusion model.** Diffusion of RNAP on DNA can be modeled as 1D
348 diffusion of a point particle with one reflecting end and one absorbing end. RNAP diffusion
349 coefficient and RNAP retention on DNA such as PIFE occurrence and start timing can be
350 estimated using this model

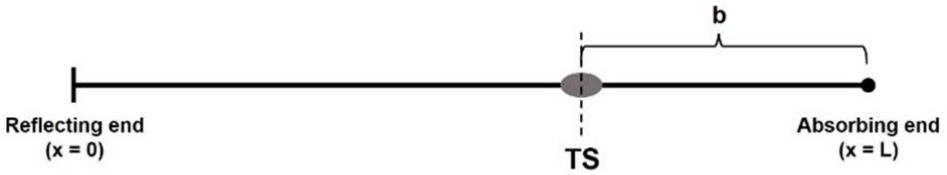

351 .
352 The mean time to reach the absorbing end, $W(x)$, is defined as a function of the distance
353 between the reflecting end and termination site (TS), x. Then, $W(x)$ satisfies the equation (1).
354 $$W(x) = \tau + \frac{1}{2}[W(x-\delta) + W(x+\delta)] \quad (1)$$

where δ is a step size of the random walk of the particle moving rightward or leftward every τ s. Because RNAP does not remain on DNA permanently, an RNAP dissociation term is added to the equation (1).

$$W(x) = \tau + \frac{1}{2}(1 - \frac{\tau}{t_{dis}})[W(x-\delta) + W(x+\delta)] \qquad (2)$$

where t_{dis} is a dissociation time of RNAP after termination. In the limit $\delta \to 0$, we can get the differential equation (3) for $W(x)$.

$$W(x) - \mathrm{t}_{dis} = \mathrm{t}_{dis} D \frac{\partial^2}{\partial x^2} W(x) \qquad (3)$$

where D is a diffusion coefficient, defined as $\delta^2/2\tau$.

When TS is positioned at the reflecting end ($x = 0$), the mean capture time does not change with x. When TS is positioned at the absorbing end ($x = \mathrm{L}$), the particle is captured right after the particle release, generating the boundary conditions (4) and (5).

$$\frac{dW}{dx}_{x=0} = 0 \qquad (4) \qquad\qquad \mathrm{W(L)} = 0 \qquad (5)$$

With these boundary conditions, the equation (3) is solved as a function of x and the total length L as shown in equation (6).

$$W(x;L) = t_{dis}\left(1 - {\cosh(x/l_D)}\Big/{\cosh(L/l_D)}\right) \qquad (6)$$

where l_D^2 is equal to t_{dis}D. Since x is fixed as 88 bp in our experiments, we can rewrite the equation (6) as a function of the distance between TS and the absorbing end, denoted by b.

$$W(b) = t_{dis}\left(1 - {\cosh(88/l_D)}\Big/{\cosh((88+b)/l_D)}\right) \qquad (7)$$

Diffusion coefficient of RNAP can be estimated by fitting PIFE timing data to the equation (7).

Similarly, the probability of capture on the absorbing end, $P(x)$, is defined as a function of x. Then, $P(x)$ also satisfies the equation (8).

$$P(x) = \frac{1}{2}(1 - \frac{\tau}{t_{dis}})[P(x-\delta) + P(x+\delta)] \qquad (8)$$

In the limit $\delta \to 0$, we can get the differential equation (9) for $P(x)$.

$$P(x) = \mathrm{t}_{dis} D \frac{\partial^2}{\partial x^2} P(x) \qquad (9)$$

When TS is positioned at the reflecting end, the probability of capture also does not change

380 with x. Otherwise, the probability of capture is equal to the RNAP retention probability
381 during termination at TS when TS is positioned at the absorbing end. These two conditions
382 generate two boundary conditions (10) and (11).

383 $$\frac{dP}{dx}_{x=0} = 0 \quad (10) \qquad \mathrm{P(L)} = y_0 \quad (11)$$

384 where y_0 is the RNAP retention probability during termination at TS. With these boundary
385 conditions, we can solve the equation (9) to get the equation (12).

386 $$P(x; L) = y_0 \, \cosh(x/l_D) \Big/ \cosh(L/l_D) \quad (12)$$

387 We can rewrite the *P*(*x*) as a function of b.

388 $$P(b) = y_0 \, \cosh(88/l_D) \Big/ \cosh((88 + b)/l_D) \quad (13)$$

389 RNAP retention probability during termination at TS can be estimated by fitting PIFE
390 occurrence to the equation (13).
391
392 **Calculation of reinitiation efficiencies.** Among the three types of fluorescence traces of Fig.
393 3C, type 3 uniquely represents TS-readthrough events (Fig. 3B), but does not cover all of
394 them because transcript probing is not complete. The unprobed readthrough events are not
395 distinguishable from non-activated events and could not be directly counted.
396 On the other hand, types 1 (0.101) and 2 (0.406) together represent total TS-
397 termination events (Fig. 3B), but their sum (0.507) is an overestimation because of
398 incomplete probing. However, using the measured termination efficiency of 33.5%, the
399 unprobed readthrough events (type 4) can be estimated to be 0.513, i.e.
400 (0.507−0.335)/0.335. Types 3 (0.493) and 4 (0.513) together represent total readthrough
401 events (1.006), with probing efficiency of 49.0%. Then, total readthrough and termination
402 events become 1.513.
403 Due to incomplete probing, some reinitiation events must have been shown as type 2
404 instead of type 1. Assuming that probing efficiency was the same in readthrough and
405 termination events, total probed and unprobed reinitiation events can be estimated to be
406 0.206 (= 0.101/0.490), and the remaining dissociation events being 0.301 (= 0.507 − 0.206).

407 Thus, the reinitiation portion among the total termination events is 40.6% (= 0.206/0.507)
408 with a mixture of holoenzymes and core enzymes.
409
410 **Acknowledgments**
411 We thank Prof. Robert Landick for plasmid pRPODS366C encoding a single-cysteine
412 derivative of σ^{70}. This work was supported by grants from the National Research Foundation
413 of Korea (2019R1A2C2005209 to SH and 2017R1A2B4002213 to JYL), the High Risk High
414 Return Project of KAIST (N10110078 to CK), and the Research Fund of UNIST (1.160106.01 to
415 JYL).
416
417 **Author contributions**
418 C.K. and S.H. conceived the study. K.S.H. constructed transcription complexes and
419 performed molecular biology experiments. W.K., H.U., K.P., and J.Y.L. measured the single-
420 molecule fluorescence images and performed biophysics experiments. C.K. supervised the
421 molecular biology part. S.H. supervised the biophysics part. All analyzed the data and
422 contributed to writing of the paper.
423
424 **Declaration of interests**
425 The authors declare no competing interests.
426
427 **References**
428 [1] Platt, T. (1986). Transcription termination and the regulation of gene expression. Ann.
429 Rev. Biochem. *55*, 339-372.
430 [2] Winkler, W.C. & Breaker, R.R. (2005). Regulation of bacterial gene expression by
431 riboswitches. Annu. Rev. Microbiol. *59*, 487-517.
432 [3] Farnham, R.J. & Platt, T. (1981). Rho-independent termination: dyad symmetry in DNA
433 causes RNA polymerase to pause during transcription in vitro. Nucleic Acids Res. *3*,
434 563-577.
435 [4] Wilson, K.S. & von Hippel, P.H. (1995). Transcription termination at intrinsic
436 terminators: The role of the RNA hairpin. Proc. Natl. Acad. Sci. USA. *92*, 8793-8797.

437 [5] Czyz, A., Mooney, A., Laconi, A., & Landick, R. (2014). Mycobacterial RNA polymerase
438 requires a U-Tract at intrinsic Terminators and is aided by NusG at suboptimal
439 terminators. mBio 5, e00931.
440 [6] Mondal, S., Yakhnin, A.V., Sebastian, A., Albert, I. & Babitzke, Paul. (2016). NusA-
441 dependent transcription termination prevents misregulation of global gene expression.
442 Nat. Microbiol. 1, 1-7.
443 [7] Gusarov, I. & Nudler, E. (1999). The mechanism of intrinsic transcription termination.
444 Mol. Cell *3*, 495-504.
445 [8] Ray-Soni, A., Mooney, R.A. & Landick, R. (2017). Trigger loop dynamics can explain
446 stimulation of intrinsic termination by bacterial RNA polymerase without terminator
447 hairpin contact. Proc. Natl. Acad. Sci. USA *114*, E9233-E9242.
448 [9] Larson, M.H., Greenleaf, W.J., Landick, R. & Block, S.M. (2008). Applied force reveals
449 mechanistic and energetic details of transcription termination. Cell *132*, 971-982.
450 [10] Hwang, H., Kim, H. & Myong, S. (2011). Protein induced fluorescence enhancement as
451 a single molecule assay with short distance sensitivity. Proc. Natl. Acad. Sci. USA *108*,
452 7414-7418.
453 [11] Bellecourt, M.J., Ray-Soni, A., Harwig, A., Mooney, R.A. & Landick, R. (2019). RNA
454 Polymerase Clamp Movement Aids Dissociation from DNA but Is Not Required for RNA
455 Release at Intrinsic Terminators. J. Mol. Biol. 431, 696-713.
456 [12] Kapanidis, A.N., Margeat, E., Laurence T. A., Doose S., Ho, S. O., Mukhopadhyay, J.,
457 Kortkhonjia, E., Mekler, V., Ebright, R.H. & Weiss, S. (2005). Retention of transcription
458 initiation factor σ^{70} in transcription elongation: single-molecule analysis. Mol. Cell *20*,
459 347-356.
460 [13] Harden, T.T., Wells, C.D., Friedman, L.J., Landick, R., Hochschild, A., Kondev, J. & Gelles,
461 J. (2016). Bacterial RNA polymerase can retain σ^{70} throughout transcription. Proc. Natl.
462 Acad. Sci. USA *113*, 602-607.
463 [14] Callaci, S., Heyduk, E. & Heyduk T. (1998). Conformational changes of Escherichia coli
464 RNA polymerase σ^{70} factor induced by binding to the core enzyme. J. Biol. Chem. *273*,
465 32995-33001.
466 [15] Epshtein, V., Toulme, F., Rahmouni, A.R., Borukhov, S. & Nudler E. (2003). Transcription

467 through the roadblocks: the role of RNA polymerase cooperation. EMBO J. *22*, 4719-
468 4727.
469 [16] Lee, J.Y., Finkelstein, I.J., Arciszewska, L.K., Sherratt, D.J. & Greene, E.C. (2014). Single-
470 molecule imaging of FtsK translocation reveals mechanistic features of protein-protein
471 collisions on DNA. Mol. Cell *54*, 832-843.
472 [17] Berg, H.C. (1983). Random Walks in Biology (New Jersey: Princeton University Press),
473 pp.37-47.
474 [18] Singer, P. & Wu, C.W. (1987). Promoter search by Escherichia coli RNA polymerase on a
475 circular DNA template. J. Biol. Chem. *262*, 14178-14189.
476 [19] Ricchetti, M., Metzger, W. & Heumann, H. (1988). One-dimensional diffusion of
477 Escherichia coli DNA-dependent RNA polymerase: a mechanism to facilitate promoter
478 location. Proc. Natl. Acad. Sci. USA *85*, 4610-4614.
479 [20] Guthold, M., Zhu, X., Rivetti, C., Yang, G., Thomson, N.H., Kasas, S., Hansma, H.G.,
480 Smith, B., Hansma, P.K. & Bustamante, C. (1999). Direct observation of one-
481 dimensional diffusion and transcription by Escherichia coli RNA polymerase. Biophys. J.
482 *77*, 2284-2294.
483 [21] Wang, F., Redding, S., Finkelstein, I.J., Forman, J., Reichman, D.R. & Greene, E.C. (2013).
484 The promoter-search mechanism of Escherichia coli RNA polymerase is dominated by
485 three-dimensional diffusion. Nat. Struct. Mol. Biol. *20*, 174-181.
486 [22] So, L., Ghosh, A., Zong, C., Sepulveda, L.A., Segev, R. & Golding, I. (2011). General
487 properties of transcriptional time series in Escherichia coli. Nat. Genet. *43*, 554-560.
488 [23] Chong, S., Chen, C., Ge, H. & Xie, X.S. (2014). Mechanism of transcriptional bursting in
489 bacteria. Cell *158*, 314-326.
490 [24] Fujita, K., Iwaki, M. & Yanagida, T. (2016). Transcriptional bursting is intrinsically
491 caused by interplay between RNA polymerases on DNA. Nat. Commun. *7*, 13788.
492 [25] Rocha, E.P.C. (2008). The organization of the bacterial genome. Annu. Rev. Genet. *42*,
493 211–233
494 [26] De, S. & Babu, M.M. (2010). Genomic neighborhood and the regulation of gene
495 expression. Curr. Opin. Cell Biol. *22*, 326–333.
496 [27] Meyer, S., & Beslon, G. (2014). Torsion-mediated interaction between adjacent genes.

497 PLoS Comput. Biol. *10*, e1003785.
498 [28] Pannier, L., Merino, E., Marchal, K. & Collado-Vides, J. (2017). Effect of genomic
499 distance on coexpression of coregulated genes in E. coli. PLoS One *12*, e0174887
500 [29] Ansari, A. & Hampsey, M. (2005). A role for the CRF 3'-end processing machinery in
501 RNAP II-dependent gene looping. Genes Dev. *19*, 2969.
502 [30] Kaderi, B.E., Medler, S., Raghunayakula, S. & Ansari, A. (2009). Gene looping is
503 conferred by activator-dependent interaction of transcription initiation and
504 termination machineries. J. Biol. Chem. *284*, 25015–25025.
505 [31] Hampsey M., Singh, B.N., Ansari, A., Laine, J.P. & Krishnamurthy, S. (2010). Control of
506 eukaryotic gene expression: gene loops and transcriptional memory. Adv. Enzyme
507 Regul. *51*, 118-125.
508
509
510 **FIGURES**
511
512 **Fig. 1. Intrinsic termination observed in single-molecule fluorescence experiments.** (**A**)
513 DNA template L+15 with T7A1 promoter and tR2 terminator was pre-labeled with biotin at
514 the upstream end and with Cy5 at the downstream end. RNA transcript was labeled with
515 Cy3 at the 5'-end. (**B**) Experimental scheme. Transcription complexes were stalled,
516 immobilized and then resumed to follow readthrough or termination pathway. (**C**) Cy3-RNA
517 and Cy5-DNA images (black) before and 10 s after NTP addition. Purple circles spot the
518 termination complexes that have lost Cy3-RNA. (**D**-**E**) Representative fluorescence traces at
519 green and red laser excitations from readthrough (D) and termination (E) complexes. Yellow
520 vertical lines indicate NTP addition timing. (**F**) Construct with Cy5 placed on σ^{70} factor. (**G**)
521 Retention of Cy5-σ on DNA after termination (top) more frequent than dissociation
522 (bottom).

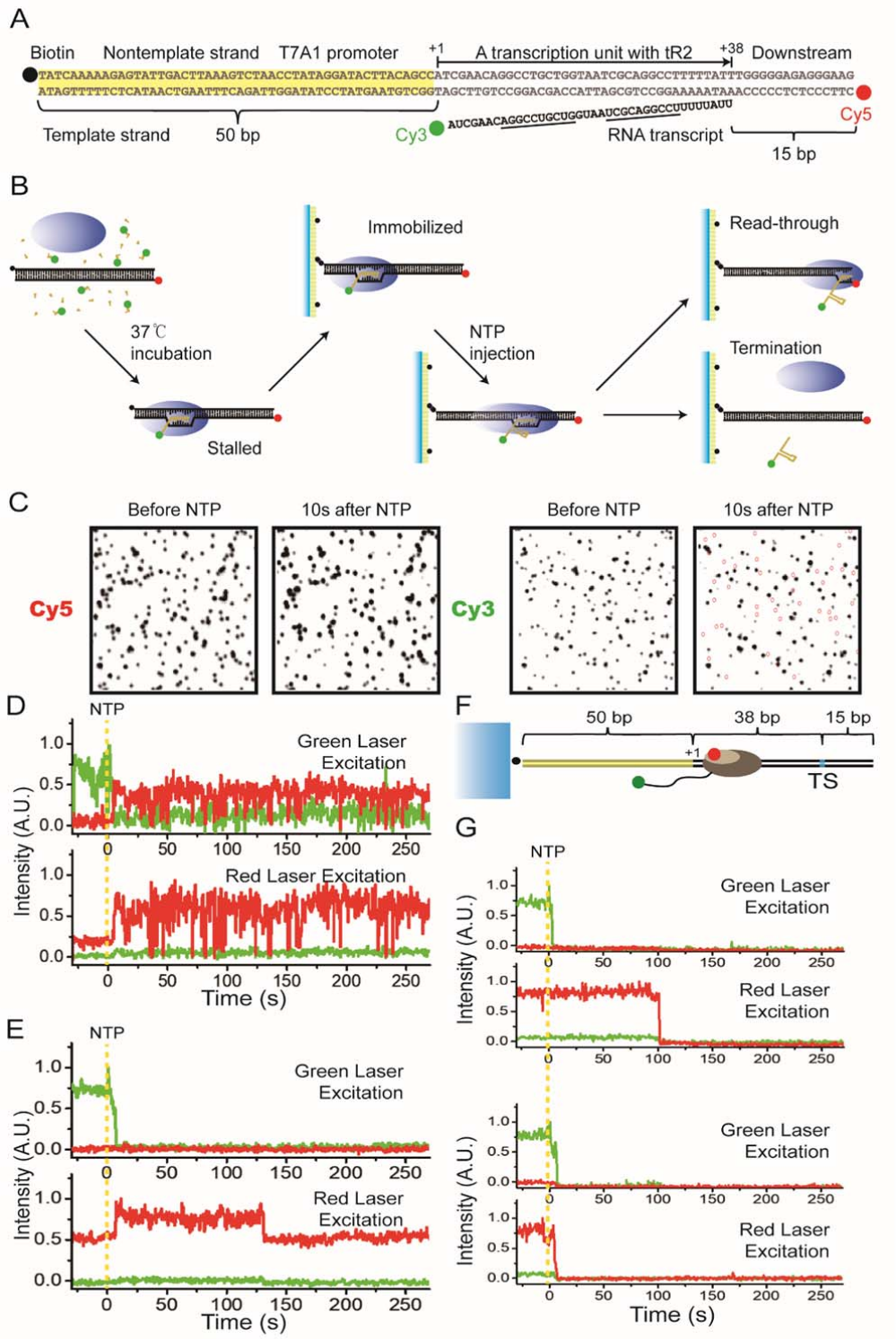
A
Biotin
Nontemplate strand
T7A1 promoter
+1
A transcription unit with tR2
+38
Downstream
Template strand
50 bp
Cy3
RNA transcript
15 bp
Cy5
B
37℃ incubation
Immobilized
Stalled
NTP injection
Read-through
Termination
C
Before NTP
10s after NTP
Cy5
Cy3
D
NTP
Green Laser Excitation
Red Laser Excitation
Intensity (A.U.)
Time (s)
E
F
50 bp
38 bp
15 bp
TS
G

523

524 **Fig. 2. Diffusion of RNAP on DNA after termination.** (**A**) DNA templates with varying
525 distance between TS (cyan) and Cy5-labeled end (red) with or without an EcoRI binding site
526 (purple). (**B**) Reduction of Cy5 PIFE occurrence by a roadblock on L+112 but not L+112R. (**C**)
527 PIFE start timings plotted against TS-end distances. Cy5 PIFE start was timed since Cy3
528 vanishing from six templates, L+15 through L+512 (black). The timing data fit to a 1D
529 diffusion model (blue). (**D**) PIFE occurrences plotted against TS-end distances. Cy5 PIFE was
530 counted with the six templates (black). The occurrence data fit to the same 1D diffusion
531 model (blue) but not a 3D diffusion model (red).

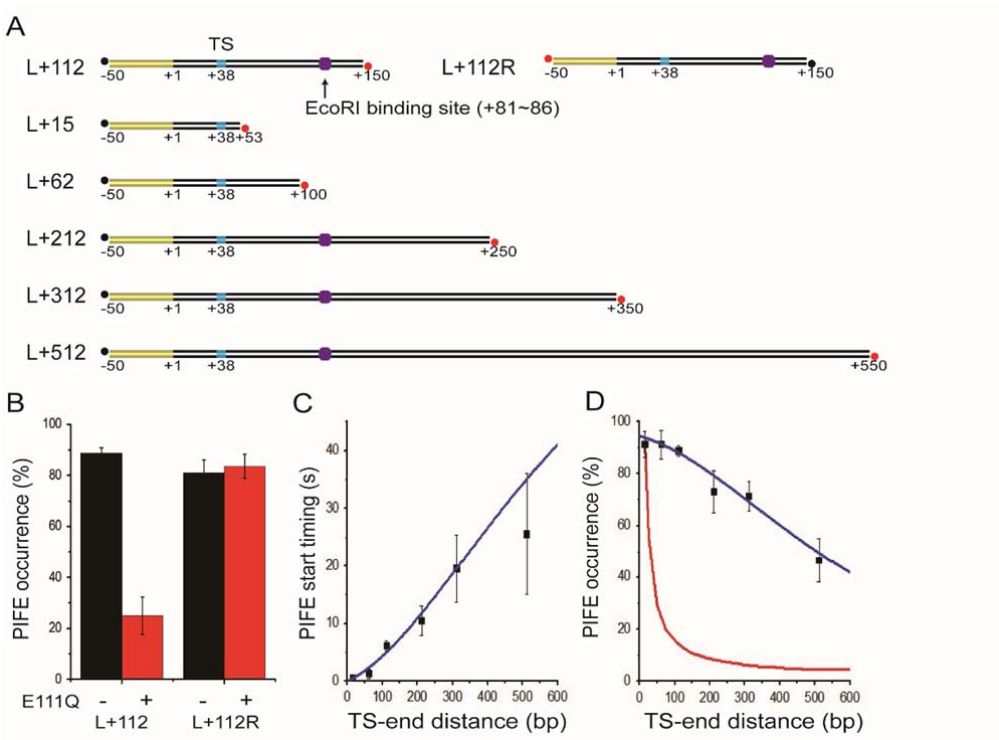

532 **Fig. 3. Detection of transcriptional reinitiation.** (**A**) A DNA template contains two
533 transcription units with a roadblock (purple) between them. Transcripts from the
534 downstream unit have a probing target (brown). (**B**) Three possible courses are reinitiation
535 on the downstream unit after TS termination, dissociation of RNAP after TS termination, and
536 readthrough at TS with continued downstream transcription. (**C**) Three types of
537 fluorescence time-traces were observed; Cy3 vanishing with Cy5 probing (type 1), Cy3
538 vanishing without Cy5 probing (type 2), and Cy3 nonvanishing with Cy5 probing (type 3).

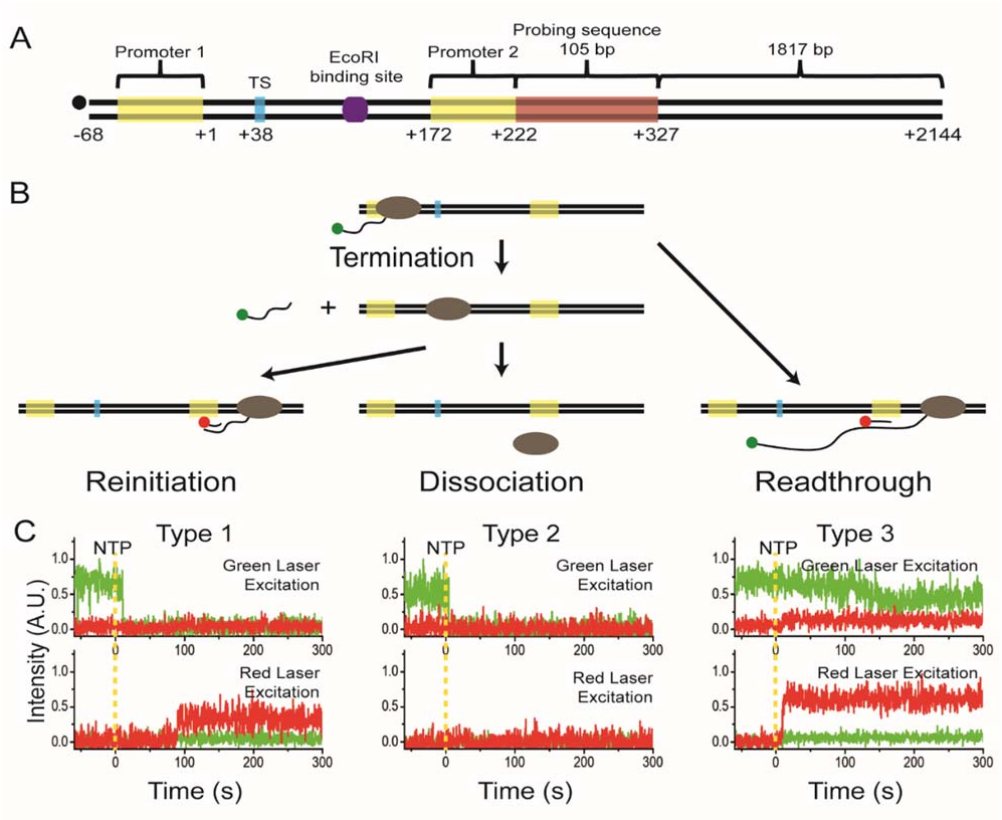
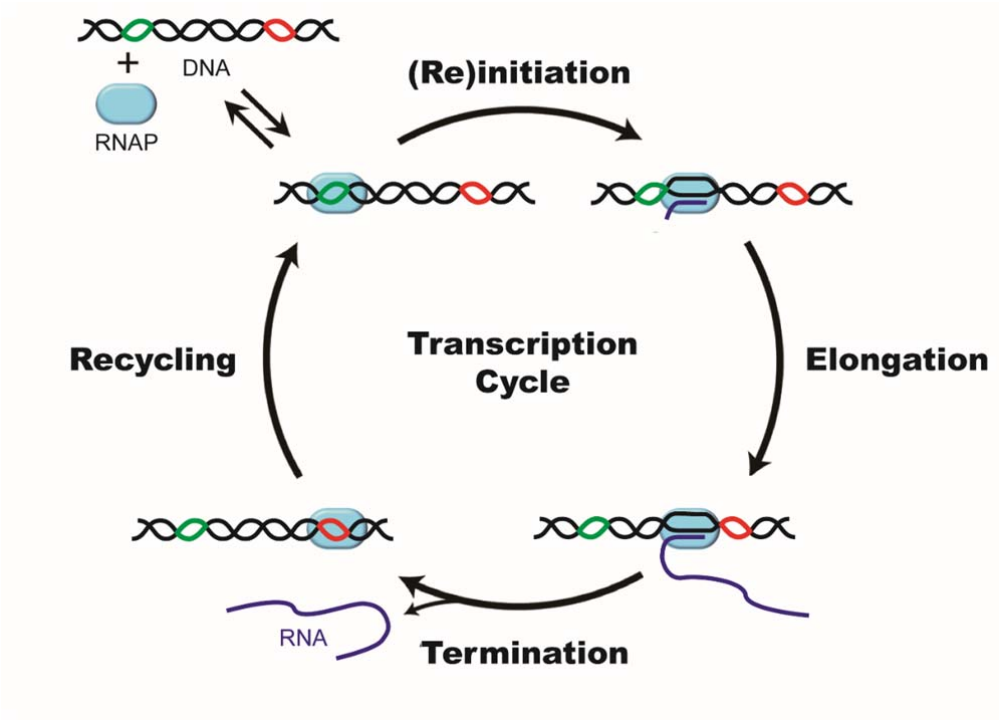
539 **Fig. 4. Four stages of transcription cycle.** (1) Initiation: After binding DNA (black) at a
540 promoter (green), RNAP (cyan) incorporates several NTPs into RNA (blue), and advances
541 downward clearing the promoter. (2) Elongation: RNAP further advances processively
542 downward, resuming from occasional pause or backtrack. (3) Termination: RNAP pauses at a
543 terminator (red) to undergo conformational changes, and releases RNA product. (4)
544 Recycling: RNAP diffuses on DNA downward and upward until it reinitiates transcription at
545 the same or another promoter unless RNAP dissociates off DNA.